3-2003

The Duration-Amplitude Distribution of Volcanic Tremor

John P. Benoit
Universtiy of Alaska Fairbanks

Stephen R. McNutt
Universtiy of Alaska Fairbanks, smcnutt@usf.edu

Vilma Barboza
National University of Costa Rica

Duration-amplitude distribution of volcanic tremor

John P. Benoit and Stephen R. McNutt
Alaska Volcano Observatory, Geophysical Institute, University of Alaska Fairbanks, Fairbanks, Alaska, USA

Vilma Barboza
Observatorio Vulcanologico y Sismologico de Costa Rica (OVSICORI), Universidad Nacional, Heredia, Costa Rica

Received 4 October 2001; revised 27 September 2002; accepted 22 November 2002; published 12 March 2003.

[1] The duration-amplitude distribution of volcanic tremor was examined in eight volcanoes and one geothermal area. An exponential model, implying a scale-bound source process, is found to be a better fit to the data than a power law (scale invariant) model. The exponential model well describes tremor associated with magmatic and phreatic eruptions, shallow and deep source regions, and geothermal sources. We tested the exponential model described by: $d(D_R) = d_t e^{-\lambda D_R}$, where d is the duration of tremor greater than or equal to a particular amplitude D_R, d_t is the total duration of tremor, and the inverse of λ is the characteristic amplitude of the distribution. λ^{-1} takes on values between 0.003 and 7.7 cm^2. Our results show that the characteristic amplitude for eruptive tremor is greater than for noneruptive tremor, that for deep tremor is greater than for shallow tremor, and that for tremor associated with magmatic eruptions is greater than for tremor associated with phreatic eruptions. The exponential scaling of tremor suggests that tremor is not simply composed of a series of low-frequency events closely spaced in time. Further, the exponential scaling requires the source to be scale bound; the amplitude variations of tremor are distributed about a constant characteristic amplitude. We propose that exponential scaling of tremor amplitude is caused by fixed source geometry driven by variable excess pressures. The exponential scaling of tremor demonstrates that tremor source processes are fundamentally different from those for earthquakes. *INDEX TERMS:* 7280 Seismology: Volcano seismology (8419); 8414 Volcanology: Eruption mechanisms; 8439 Volcanology: Physics and chemistry of magma bodies; 8494 Volcanology: Instruments and techniques; *KEYWORDS:* scaling, volcanic tremor, exponential model, power law model, duration-amplitude

Citation: Benoit, J. P., S. R. McNutt, and V. Barboza, Duration-amplitude distribution of volcanic tremor, *J. Geophys. Res.*, *108*(B3), 2146, doi:10.1029/2001JB001520, 2003.

1. Introduction

[2] Most phenomena in nature show systematic relationships between their numbers and their sizes. Thus, the measurement and modeling of the scaling or frequency of occurrence versus size distribution provides a simple means to begin to understand the source processes underlying a phenomenon. (A note on terminology: scaling is the general term, frequency-size or frequency-magnitude is used for discrete phenomena such as earthquakes, and duration-amplitude for continuous phenomena).

[3] An understanding of scaling may provide important physical constraints on theoretical source models. For instance, in earthquakes studies, the frequency-size distribution is well described by a power law [e.g., *Ishimoto and Ida*, 1939; *Gutenberg and Richter*, 1954]. This observation has lead to several insights into the earthquake source process, for example, stress drop is relatively constant and independent of earthquake size [*Aki*, 1972; *Kanamori and Anderson*, 1975]. Additional physical implications can be derived from an examination of variations in the frequency-size distribution (i.e., variations in b-value). Some of these include; the stress drop involved during rupture [*Wyss*, 1973], the applied stress [*Scholz*, 1968], the temperature gradient [*Warren and Latham*, 1970] and the heterogeneity of the medium [*Mogi*, 1962]. The scaling of earthquakes or "b-value," is the second most widely studied parameter in seismology [*Bath*, 1981]. In contrast, the amplitude scaling of volcanic tremor has received very little attention in the literature.

[4] In this study we investigate the scaling relationships between the duration of volcanic tremor and its amplitude in 8 volcanoes: Kilauea (Hawaii), Mt. Spurr, Pavlof, and Redoubt (Alaska), Karkar, Ulawun (Papua New Guinea), Fuego (Guatemala), and Arenal (Costa Rica). The tremor from these volcanoes is associated with a range of different volcanic phenomena. A case from a geothermal area, Old Faithful Geyser (Yellowstone National Park), and a swarm of long-period earthquakes from Redoubt volcano are also studied for comparison.

[5] *Aki and Koyanagi* [1981] were the first to demonstrate an exponential distribution for the duration-amplitude

0148-0227/03/2001JB001520$09.00

distribution of tremor at one location. They found that for deep ($\geq$30 km) tremor at Kilauea an exponential law applies rather than a power law, and they postulated that there is a unique length scale involved in the source process of volcanic tremor, such as the average size of the conduits. *McNutt* [1992] expanded this work by comparing data from Kilauea with Pavlof, and showed that the scaling is similar at these two volcanoes. In this paper we extend these results to 8 volcanoes and examine the implications for the source processes.

2. Frequency-Size Distributions

[6] Power law and exponential distributions are among the most commonly used distributions to describe frequency-size relations in geophysics. They also provide a good contrast between scale invariant and scale bound distributions. The power law is the only distribution that does not include a characteristic scale length [e.g., *Turcotte*, 1992]. In contrast, the exponential distribution is one of several distributions, such as the gamma and Weibull, which are bounded about a mean or characteristic size. We chose the exponential distribution for further examination because it is perhaps the simplest; it can be described by a single-parameter; and it provides a good starting point with which to compare scale invariant and scale bound processes.

[7] A power law describes source processes for which no characteristic scale is involved, or, in other words, the source processes are self-similar. For example, the frequency-size distribution for earthquakes [e.g., *Ishimoto and Ida*, 1939; *Gutenberg and Richter*, 1954], faults [e.g., *Okubo and Aki*, 1987], rock fragments (e.g., volcanic ash and pumice) [*Hartman*, 1969], and volcanic eruptions [*Simkin*, 1993] are all adequately described with a power law model. In contrast, however, the exponential distribution describes phenomena where the source process is scale-bounded. For example, fault blocks [*Korvin*, 1989], volcano spacing [*Vogt*, 1974], and seamount heights [*Smith and Jordan*, 1987] are well described with exponential distributions.

[8] The mean of an exponential distribution completely describes the distribution and can have implications for source processes. The mean of the exponential distribution is also referred to as the characteristic size. For fault blocks at crustal scale and volcano spacing, the characteristic size is essentially equal to the thickness of the lithosphere [*Korvin*, 1989; *Vogt*, 1974]. Similarly, the characteristic length associated with contraction-crack polygons has been related to the elastic properties and thickness of the contracting layer [e.g., *Neal et al.*, 1968]. Seamount height studies have shown that the characteristic length is consistent with the depth of a magma source at the base of the oceanic crust [*Smith and Jordan*, 1987].

[9] Recently, power law scaling has received a great deal of attention because of its broad application to geological data, and to chaos theory [e.g., *Korvin*, 1989; *Turcotte*, 1992]. Several authors have applied a power law scaling to describe the frequency-magnitude relation for low-frequency, long-period, or b-type volcanic events, hereafter referred to as low-frequency events [e.g., *Minakami*, 1960; *Shimozuru and Kagiyama*, 1989]. Hence, if volcanic tremor is the superposition of low-frequency events [e.g., *Fehler*, 1983] then the duration-amplitude distribution for tremor should also exhibit power law scaling [*Nishimura*, 1995]. We test this hypothesis at several different volcanoes for which we have high quality data on the durations of tremor for different amplitudes, and by using synthetic data. If, on the other hand, low-frequency events are produced by geometrically bounded structure such as the average size of cracks or conduits, an exponential distribution may be a more appropriate distribution to describe the duration-amplitude relation. This should be evident from comparing plots of linear duration versus log amplitude to plots of log duration versus log amplitude.

3. Methods

[10] The determination of the frequency-size distribution, for discrete events, requires only the counting of events of a particular size and then plotting their numbers versus their size. Volcanic tremor, a continuous signal, requires a different approach. In order to determine the frequency of occurrence or event count for tremor we use the tremor duration as an analog. The tremor duration at a particular amplitude or greater is then measured. An example measurement is shown in Figure 1 for tremor associated with the 27 December 1996 eruption of Pavlof volcano. Three techniques were used to measure tremor durations; the first was by simply using a scale (ruler) and directly measuring the duration from an existing figure; the second was the processing of digital Real-time Seismic Amplitude Measurement (RSAM) data [*Endo and Murray*, 1991]; and the third was the automatic calculation of amplitudes and durations in near-real-time using the Iceworm seismic acquisition system [*Lindquist et al.*, 1997]. When sufficient accessory information was available, tremor amplitudes are reported as reduced displacements (D_R). Reduced displacement for volcanic tremor is a normalized amplitude metric, analogous to the magnitude scale for earthquakes. The D_R accounts for the instrument magnification, distance to the source, and the type of waves composing the tremor. The definition of D_R is given in Appendix A. Using this normalized standard allows comparison of tremor amplitudes at many volcanoes.

[11] Numerous plots of tremor amplitude verses time exist in the literature. The frequency-size distribution can be easily determined by measuring durations from these figures using a scale. Figure 1 shows a measured duration of 46 hours for tremor amplitude greater than or equal to a reduced displacement of 5 cm^2. This duration is then plotted against amplitude to examine the form of the duration-amplitude distribution. This technique allows a broad spectrum of tremor from several volcanoes to be analyzed, however, this technique is quite time consuming.

[12] When primary or derivative amplitude data (e.g., RSAM data) are available, these data sources were used instead. The duration-amplitude distribution can be directly measured using RSAM data of tremor episodes. RSAM data are 1-minute averages of the absolute value of signal amplitude [*Endo and Murray*, 1991] and the final recorded output is a 10-minute average of the 1-minute averages (J. Power, personal communication, 1995). Tremor durations are measured by producing a histogram of the RSAM values and tallying the number of occurrences greater than a specific amplitude. The number of occurrences is then

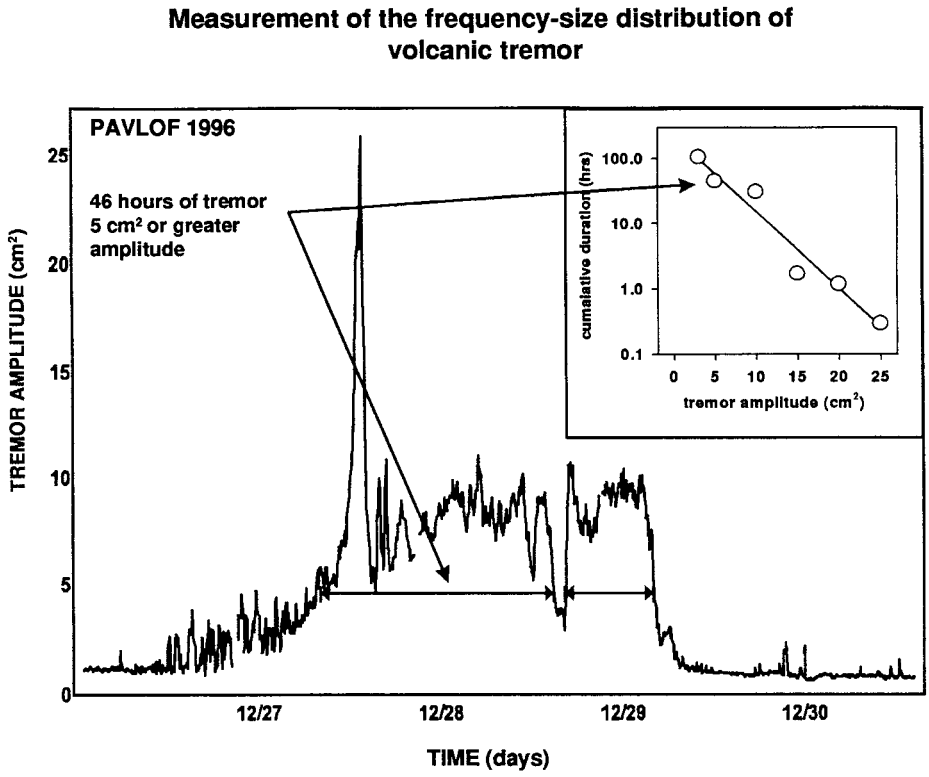

Figure 1. Measurement of the frequency-size or duration-amplitude distribution for volcanic tremor. Since tremor is a continuous signal, the duration is taken as the frequency of occurrence and the size is measured as the amplitude. An example of the duration-amplitude measurement for tremor recorded at Pavlof volcano between 26 and 30 December is shown. The inset shows the duration-amplitude distribution for this time period with a fit to an exponential scaling model.

proportional to the duration because each occurrence represents the same duration: 10 min of signal. This algorithm does an excellent job of quickly determining the durations and allows one or more tremor episodes to be analyzed together or separately. This technique gives, within measurement errors, the same results as the hand measurements from a figure using a scale. A drawback of using the RSAM data is the indiscriminate inclusion of nontremor signals such as teleseisms, regional earthquakes, microseisms, wind noise, and seismometer calibration pulses. The data must be carefully screened for these types of signals before amplitude-duration measurements are made.

[13] Near-real time tremor duration-amplitude measurements were made using the Iceworm data acquisition system during the 1996 eruption of Pavlof volcano [*Lindquist et al.*, 1997]. The amplitude of the tremor is measured in the frequency domain, to minimize nonvolcanic signals such as wind noise and microseisms. Spectra are calculated for 10-second windows with 50% overlap and then averaged over 15 min. The maximum spectral amplitude is taken between 0.8 and 10.0 Hz, which essentially acts as a bandpass filter to minimize energy from microseisms (<0.8 Hz) and wind noise (>10 Hz). The spectral amplitude is converted to an RMS ground displacement using Parseval's identity and accounting for the instrument response. The D_R is then calculated by incorporating the station-vent distance to correct for geometrical spreading (see Appendix A). Results from this technique are comparable to the above methods.

[14] We fitted both power law and exponential models to each of the duration-amplitude distributions. Figure 2 shows a comparison of these models for noneruptive tremor recorded at Mt. Spurr volcano. Figure 2a shows a plot of $\log_{10}$ tremor duration versus "linear" amplitude. The line is a weighted-least-squares fit corresponding to an exponential distribution of the form

$$d(D_R) = d_t e^{-\lambda D_R} \quad (1)$$

where D_R, is the tremor amplitude, d is the total duration of tremor with amplitudes greater than or equal to D_R, d_t is the total duration of tremor during the period studied, and λ is the slope of the line or scaling parameter. The inverse of the scaling parameter, λ^{-1}, can be thought of as the characteristic or mean amplitude of the distribution. Figure 2b shows a plot of log tremor duration versus log amplitude. The line is a weighted-least-squares fit to a power law distribution in the form

$$d(D_R) = d_t(D_R)^{-\gamma} \quad (2)$$

where γ is the is the slope of the line, similar to the "b-value" for earthquakes. The parameter γ also can be related to the fractal dimension of the amplitudes.

[15] Visual inspection of Figure 2 immediately shows that the exponential model is a better fit than the power law

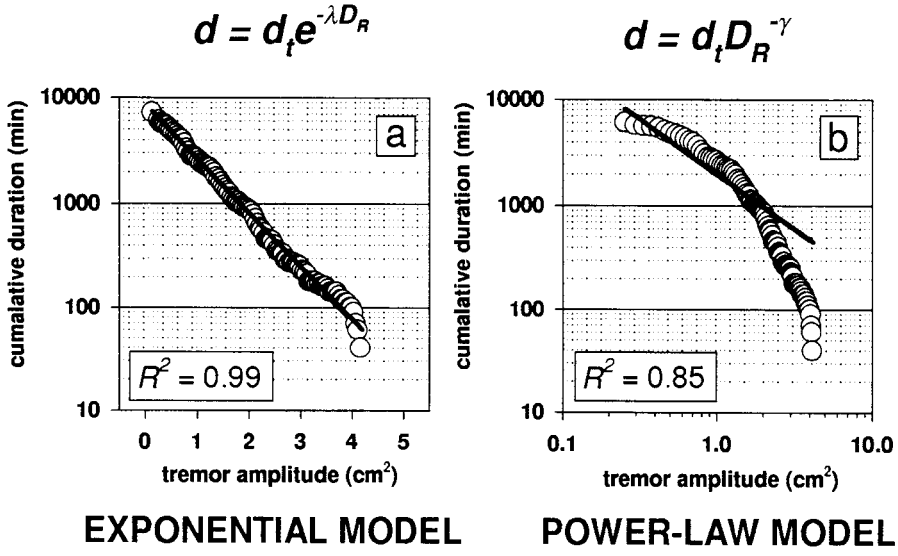

Figure 2. Comparison between an exponential and a power law scaling model for the duration-amplitude distribution of volcanic tremor. The lines shown through the data are weighted-least-squares fits to exponential and power law models. These data are from a noneruptive tremor sequence recorded at Mt. Spurr volcano.

model. Two methods are employed to establish a formal goodness-of-fit between these models and the data. The first test is a comparison of the correlation coefficients (R^2) of the linear regressions for both models. The correlation coefficient is a measure of variability about the modeled distribution and higher values are found for better fits. Correlation coefficients of 0.99 and 0.85 are calculated for the exponential and power law models, respectively. In other words, the exponential model accounts for 99% of the variability in the distribution, whereas the power law models accounts for only 85%. For the Mt. Spurr case and all other cases studied, the exponential model is found to have higher correlation coefficients, and therefore, is considered to be superior to the power law.

[16] A second formal method, the chi-square test (X^2), was also used to test the goodness-of-fit for both models for selected cases. The hypothesis tested is; the duration sample was randomly drawn from either an exponential or a power law distribution. These hypotheses can be rejected if the X^2 statistic is greater than a critical value. The X^2 statistic is defined by

$$\mathrm{X}^2 = \sum_{i=1}^{n} \frac{(O_i - E_i)^2}{E_i} \tag{3}$$

where n is the number of sample classes, O_i is the observed frequency, and E_i the expected frequency as calculated by the power law or exponential models. The critical value ($X^2_{\nu,p}$) is found in published tables and depends on the number of degrees of freedom (ν) and the confidence level (p) at which the test is performed. The degrees of freedom are defined by the number of observations minus one ($n - 1$) minus the number of parameters being estimated (one parameter for the both exponential and power law models; e.g., Mt. Spurr case $\nu = (97 - 1) - 1 = 95$). For the Mt. Spurr case, the X^2 statistics for the exponential and power law models, 0.599 and 11.144 respectively, are both less than the critical value of $X^2_{95,0.975} = 130$. Therefore, we are unable to reject formally either model at the 97.5% confidence level. However, the X^2 statistic for the power law model is substantially greater than the X^2 statistic for the exponential model, showing that the exponential model is a superior fit. Similar results were obtained for the Karkar case; $\nu = 9$, $X^2 = 0.223$ for exponential model and 2.779 for power law model, and $X^2_{95,0.975} = 19.02$. For all the cases studied, the exponential model has higher correlation coefficients (R^2) and lower X^2 statistics than the power law model. Note, however, that the tests do not reject a model per se; they only associate a degree of confidence with each. We then interpret the model with the higher confidence limits to be the best representation of the data.

4. Case Studies

[17] The duration-amplitude distributions of 10 episodes of tremor in 8 volcanoes are examined in the following section. These case studies were chosen to given a broad sample of tremor associated with a suite of different volcanological processes. At Mt. Spurr we compare eruptive and noneruptive tremor. At Kilauea we examine shallow (<2 km) tremor associated with the 1983 eruptions of Pu'u O'o, and deep tremor (≥30 km) recorded between 1962 and 1979. In Papua New Guinea, Karkar and Ulawun give a comparison between tremor associated with phreatic and magmatic eruptions. Four other cases from Fuego, Arenal, and Pavlof are shown to further generalize these observations. Finally, two "nontremor" cases are presented for comparison; a long-period swarm of earthquakes at Redoubt and geothermal "seismic noise" at Old

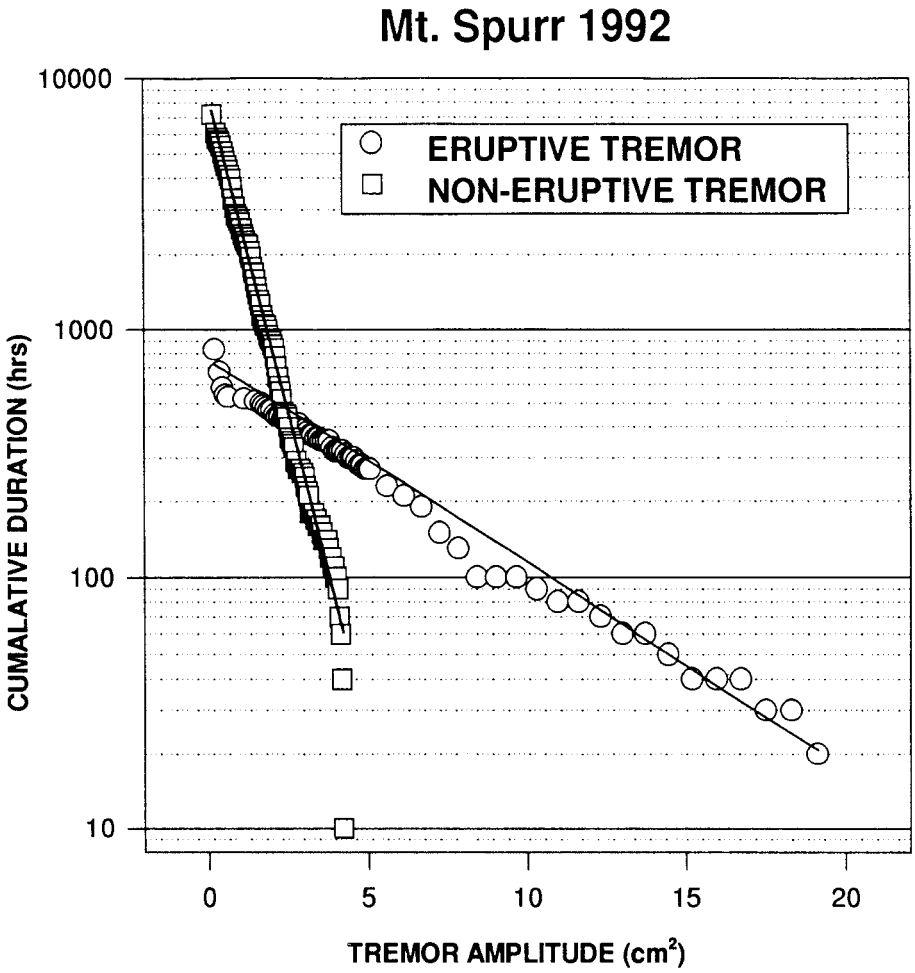

Figure 3. Tremor duration-amplitude distribution for Mt. Spurr. Two periods are shown; tremor associated with the eruption of 16–17 September 1992 (open circles) and tremor occurring between 2 and 7 October 1992 (open squares). Both distributions are well modeled with an exponential distribution. Note the difference in slope between the eruptive and noneruptive tremor.

Faithful Geyser. Details on how the durations and amplitudes were measured are presented for each case along with a summary of the volcanic activity occurring during the observations.

4.1. Crater Peak, Mt. Spurr Alaska

[18] Volcanic tremor preceded the first eruption of Crater Peak, a satellite cone of Mt. Spurr, on 27 June 1992, accompanied the 27 June, 18 August, and 16–17 September eruptions, and followed the 17 September eruption [*McNutt et al.*, 1995]. The tremor sequences between 16 September and 10 October are chosen for study because they include the last eruption as well as several episodes of continuous tremor not associated with an eruption. Five seismic stations were recording RSAM data during this period. Here, we examine RSAM data from one station, CKN, because it had the best signal-to-noise ratio of the available stations. The other stations all showed similar results. Station CKN is 6.3 km south-southeast from the eruptive vent.

[19] Tremor durations and normalized amplitudes were estimated from the RSAM data. Two periods were studied in detail; 24 hours surrounding the 16–17 September eruption, and a six-day period (2–7 October) including several episodes of noneruptive tremor.

[20] The 16–17 September eruption lasted about 3.5 hours and sent an ash plume to an elevation of 14 km above sea level. Several pyroclastic flows were generated and some entrained snow to become lahars. The erupted volume of tephra was estimated to be 20×10^6 m^3 DRE (Dense Rock Equivalent) [*Neal et al.*, 1995]. The duration-amplitude distribution for the tremor associated with this eruption is shown in Figure 3 with a weighted-least-squares fit to the exponential model. The individual measurements are shown as open circles. The correlation coefficients for the power law and exponential models are 0.73 and 0.99, respectively (Table 1). This shows that the exponential model is superior to the power law in modeling the duration-amplitude distribution. The inverse of the slope or characteristic amplitude is 5.6 cm^2 (Table 2). These parameters are summarized in Table 2 for Spurr and all other cases for which information was available to calculate normalized amplitudes.

[21] Inspection of the lowest amplitudes of the eruptive tremor distribution shows a departure in slope. The slope is

Table 1. Goodness of Fit as Measured by the Correlation Coefficient R^2 for the Exponential and Power Law Models

Case	n	R^2 (Exponential Model)	Significance Level, %	R^2 (Power Law Model)	Significance Level, %
Spurr 1992 eruptive	97	0.99	>99	0.73	>99
Spurr 1992 noneruptive	91	0.99	>99	0.85	>99
Kilauea shallow	5	0.98	>99	0.79	>99
Kilauea deep	5	0.99	>99	0.70	~98
Karkar 1978–1979	8	0.97	>99	0.59	~99
Ulawun 1978	8	0.98	>99	0.84	>99
Pavlof 1973–1986	6	0.96	>99	0.84	>99
Pavlof 1996	6	0.94	>99	0.86	>99
Arenal 1993	5	0.95	>99	0.90	>99
Fuego 1973	6	0.99	>99	0.83	>99
Redoubt 1989	6	0.95	>99	0.88	>99
Old Faithful 1972	20	0.99	>99	0.95	>99

much steeper than the eruptive tremor distribution and is similar to the noneruptive tremor distribution. These points at the lowest amplitudes represent a break in scaling and probably represent a second tremor-generating process occurring at the lowest amplitudes. The eruption tremor lasted for only 3.5 hours of the full 24 hours analyzed, thus, we may not have completely isolated the eruption tremor from a secondary source. The result is a mixture of these two distributions. The few points at the lowest amplitudes have a negligible effect on either the correlation coefficients or the calculation of the characteristic amplitude.

[22] Tremor continued for one week following the 17 September eruption and ceased on 25 September [*McNutt et al.*, 1995]. The tremor resumed on 1 October. The tremor sequence showed significant temporal variations, including patterns similar to those that have preceded eruptions at Mt. Spurr and elsewhere. Tremor starting on 1 October increased nearly exponentially on 2 October, after which is stopped rather abruptly. On 3 October a series of five tremor episodes occurred, each about 1.5 hours long. This signal resembled banded tremor. On 4 October, tremor returned and the amplitude again increased nearly exponentially. When this tremor declined in amplitude on 5 October, another series of episodes occurred, each about 2 hours long, similar to those on 3 October, but followed by a gradual decline. The duration-amplitude measurements for 2–7 October are shown in Figure 3. The individual measurements are shown as open squares.

[23] The data in Figure 3 are fit well by weighted-least-squares regression to an exponential model. The correlation coefficients are 0.85 and 0.99 for the power law and exponential models, respectively (Table 1), again demonstrating a better fit with the exponential model. Inspection of the highest amplitudes of the noneruptive tremor distribution shows a departure in slope. The slope is much steeper than the majority of the distribution. These points at the highest amplitudes represent a break in scaling and may denote an upper bound for noneruptive tremor. There is a significant difference in the slope between the eruptive and noneruptive tremor. The characteristic amplitude for the noneruptive tremor is 0.8 cm^2 (Table 2). This is the smallest characteristic amplitude for any true volcanic tremor in this study. Note that the slope of the noneruptive tremor is similar to that of the leftmost points of the eruptive tremor (those below the scale break).

4.2. Kilauea, Hawaii

[24] Tremor from shallow (<2 km) and deep (≥30 km) source regions are examined at Kilauea volcano. Data for the shallow tremor duration-amplitude distribution are drawn from measurements of the 2–11 January 1983 eruption of Pu'u O'o (episode 1) [*Koyanagi et al.*, 1989]. The Pu'u O'o eruption began as linear lava fountains from a fissure several hundred meters long, on a segment of the East Rift Zone 1 km in length. The total volume erupted during this episode was estimated to be 4.0×10^6 m^3 at an average rate of 1.1×10^6 m^3/hour [*Wolfe et al.*, 1989]. The duration and amplitude measurements were made using a scale on published histograms of tremor amplitude at station MPR, approximately 6 km from the tremor source [*Koyanagi et al.*, 1989]. The amplitudes were normalized to reduced displacement using a surface-wave formulation [*Felher*, 1983] (using the following parameters: predominant tremor frequency = 3 Hz; wave speed = 2 km/s; source-receiver distance = 6 km). The duration-amplitude distribution is shown in Figure 4. Individual measurements are

Table 2. Slope of the Duration-Amplitude Distribution Curve (λ) and Characteristic or Mean Amplitude (λ^{-1}), Determined Using a Weighted-Least-Squares Regression

Case	Maximum Amplitude, cm^2	λ, cm^{-2}	λ^{-1}, cm^2	Associated Volcanic Activity
Kilauea 1962–1979 deep	64	0.13	7.7	quiescence and varied activity at the surface
Spurr 1992 eruptive	19	0.18	5.6	sub-Plinian eruption
Pavlof 1973–1986	18	0.19	5.3	lava fountaining; Strombolian explosions
Pavlof Dec. 1996	25	0.22	4.5	lava fountaining; Strombolian explosions
Kilauea 1983 shallow	9	0.44	2.3	fissure eruption; lava fountaining
Redoubt 1989	2.5	0.74	1.4	precursory LF earthquake swarm
Spurr 1992 noneruptive	4	1.18	0.8	posteruption tremor
Old Faithful 1972	0.03	340	0.003	geysering; hydrothermal boiling

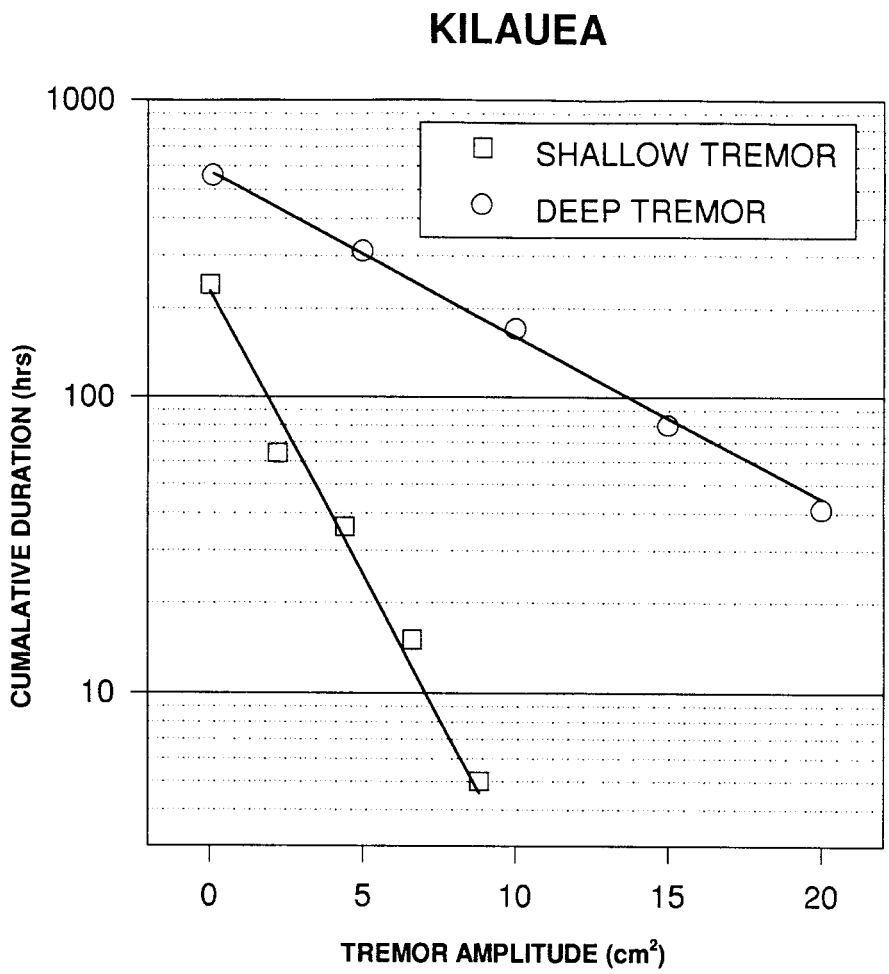

Figure 4. Duration-amplitude distribution for shallow (open squares) and deep (open circles) tremor at Kilauea volcano. The shallow tremor was recorded during the first episode the Pu'u O'o eruption in 1983. The deep tremor was recorded between 1962 and 1979. Note the difference in the slope, or characteristic amplitude, for the shallow and deep tremor.

shown as open circles and the line is a weighted-least-squares fit to the exponential model. The correlation coefficients for the power law and exponential models are 0.79 and 0.98, respectively (Table 1). The characteristic amplitude is 2.3 cm^2 (Table 2).

[25] Amplitude-duration measurements for the deep ($\geq$30 km) tremor at Kilauea were drawn directly from *Aki and Koyanagi* [1981, Table 5]. Deep tremor was distinguished from shallow tremor by its spatial amplitude distribution. The deep tremor shows uniform amplitudes at many stations over a large area and the frequencies were usually 3 to 5 Hz. Some of the deep tremor has been located at depths of 30–50 km. Duration-amplitude measurements cover an 18-year period between 1962 and 1979. These data are plotted along with the shallow tremor in Figure 4. This period included several episodes of quiescence and varied eruptive activity at the surface. During this period approximately 570×10^6 m^3 of lava was erupted at the surface. As noted by *Aki and Koyanagi* [1981], the duration-amplitude is well fit by an exponential distribution. The correlation coefficients are 0.70 and 0.99 for the power law and exponential models, respectively (Table 1). The characteristic amplitude for the deep tremor is 7.7 cm^2, which is somewhat larger than the shallow tremor (2.3 cm^2, Table 2).

4.3. Karkar and Ulawun, Papua New Guinea

[26] Tremor amplitude-duration measurements for Karkar volcano, were made for a 6-month long tremor sequence that preceded a series of phreatic eruptions in 1979. Using a scale, the amplitude-duration measurements were made from figure given by *McKee et al.* [1981a, Figure 4] showing tremor amplitudes recorded from July to December 1978, at a seismic station approximately 12 km from the eruptive vent. The tremor during this period showed intervals of stronger and weaker tremor giving the seismograms a characteristic banded appearance. The banded tremor was most noticeable for the period between July and early October 1978 and during the eruptions. Resistivity and self-potential electrical surveys provided evidence for the existence of 100–200 m-deep body of hot aquifer, which is

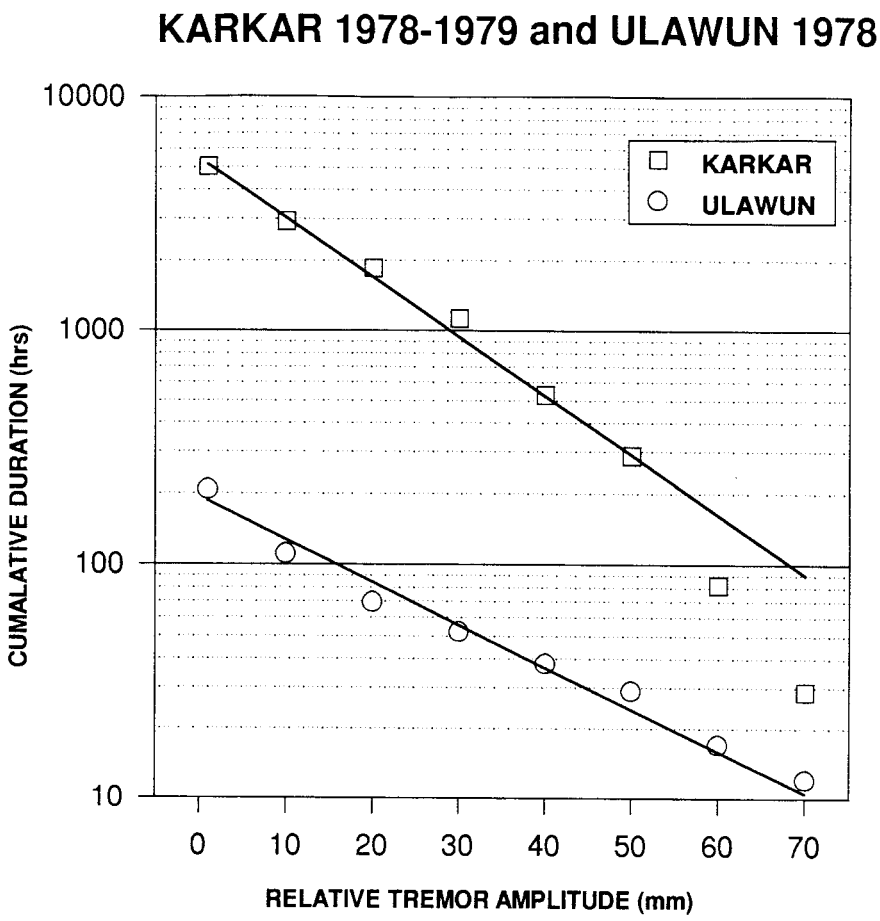

Figure 5. Duration-amplitude distribution for tremor associated with the phreatic explosions at Karkar in 1978–1979 (open squares) and the magmatic eruption at Ulawun in 1978 (open circles). Note the difference in slopes between tremor associated with a series of phreatic explosions and a magmatic eruption.

believed to be the focus of the phreatic explosions. However, the explosions could also have been gas driven. No unambiguous juvenile material was detected in the ejecta produced by the 1978–1979 explosions [*McKee et al.*, 1981a].

[27] The duration-amplitude measurement data are shown as open squares in Figure 5. An exponential model is fit through the data by a weighted-least-squares regression. The correlation coefficients for the power law and exponential models are 0.59 and 0.97, respectively, again showing that the exponential model is a superior fit (Table 1).

[28] Tremor amplitude-duration measurements for Ulawun volcano, were made for a 9-day long tremor episode that accompanied a week-long magmatic eruption in 1979. The eruption consisted of, first, ash ejection from the summit crater, second, expulsion of pyroclastic flows from a new fissure, and, finally, fountaining and flow of lava from a new fissure low on the flank. Tremor was recorded on a seismic station approximately 10 km northwest of the volcano's summit and 15 km from the site of the flank eruption. Tremor amplitudes reached a maximum the day before the formation of the fissure high on the southeastern flank. These eruptions produced an estimated 20×10^6 m^3 of tephra and $7.2–9.0 \times 10^6$ m^3 of lava [*McKee et al.*, 1981b].

[29] Using a scale, the duration-amplitude measurements were made from a figure given by *McKee et al.* [1981b, Figure 3] and are shown in Figure 5. The individual duration-amplitude measurements are shown as open circles and the line is a weighted-least-squares fit to the exponential model. The correlation coefficients for the power law and exponential models are 0.84 and 0.98, respectively (Table 1).

[30] Unfortunately, absolute amplitude units were not available for the Karkar and Ulawun tremor data. Nonetheless, Figure 5 shows a clear difference in the slopes or characteristic amplitudes for the Karkar and Ulawun duration-amplitude distributions. The characteristic amplitude for tremor associated with the magmatic eruptions is greater than that for the tremor associated with the phreatic or gas driven explosions.

4.4. Pavlof, Alaska

[31] The data presented for Pavlof are gathered from two data sets. The first data set is from tremor accompanying several eruptions that occurred between 1973 and 1986 [*McNutt*, 1987, 1986]. The eruptions primarily consisted of lava fountaining and Strombolian explosions. The second data set is from the tremor sequence that accompanied the

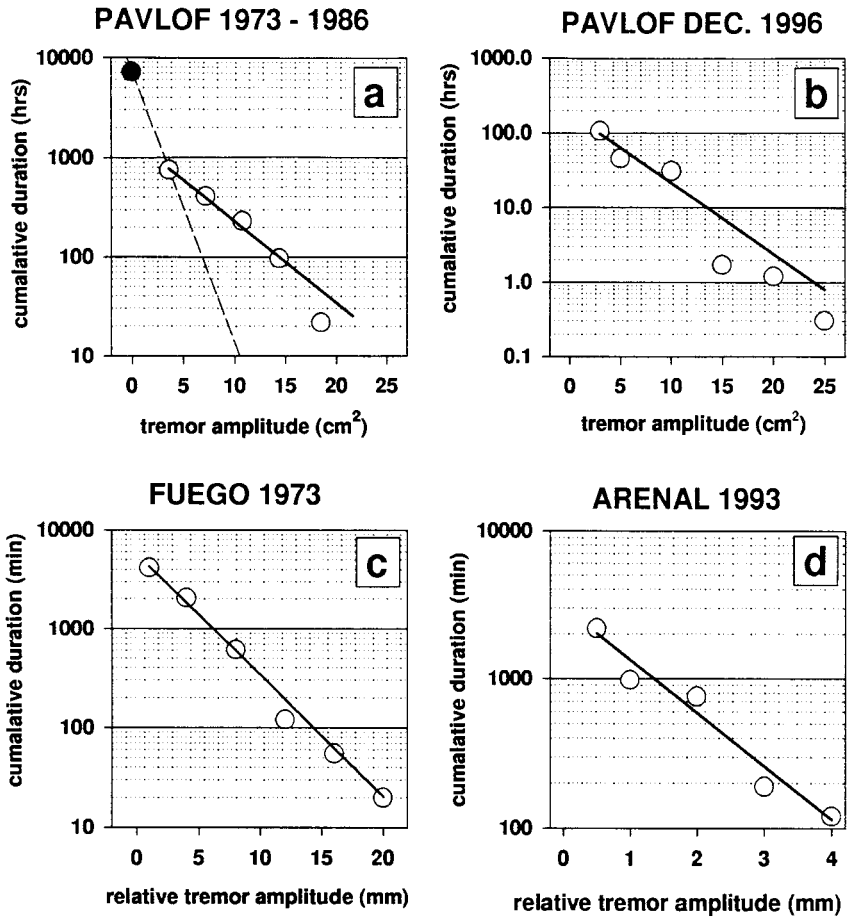

Figure 6. Duration-amplitude distribution for Pavlof 1973–1986 (a), Pavlof, December 1996 (b), Fuego (c), and Arenal (d) volcanoes. The distributions for Pavlof 1973–1986 (a) and for 1996 (b) show very similar slopes or characteristic amplitudes. The solid circle point (a) was excluded from the regression. This break in scaling suggests a mixture of more than one process generating the tremor. Duration-amplitude distributions are shown from Fuego (c) and Arenal (d) to further generalize the result that tremor is adequately described by an exponential model.

last eruptive episode of the 1996 eruption (Figure 1). For the 1973–1986 data set, amplitudes and durations were scaled off helicorder records from seismic station PVV, 8.5 km from the eruptive vent. The resulting duration-amplitude distribution is plotted in Figure 6a. An exponential model was fit to all the data except the point representing the lowest amplitudes (shown as a filled circle). This point represents a break in the scaling, and, like the Spurr case, probably represents a second tremor-generating process occurring at low amplitudes. A weighted-least-squares regression, through only the open circles, yields a characteristic amplitude of 5.3 cm^2. A comparison of the correlation coefficients (R^2 = 0.84 for the power law and R^2 = 0.96 for the exponential) again shows the exponential model to be a superior fit over the power law model (Table 1).

[32] The 1996 eruptions were, in general, very similar to the eruptions of the previous 23 years and consisted primarily of lava fountaining and Strombolian explosions. Durations and amplitudes were measured for this eruption in near-real time using the Iceworm seismic data acquisition system [*Lindquist et al.*, 1997]. The results are shown in Figure 6b. As for the other cases, the correlation coefficients show that the exponential model (R^2 = 0.94) fit the data better than the power law (R^2 = 0.86; Table 1). The characteristic amplitude for the 1996 eruptions is 4.5 cm^2. This is very similar to the characteristic amplitude of 5.3 cm^2 for tremor recorded over the previous 23 years (Table 2). The duration-amplitude distribution was changed very little even though the structure of the vent was modified somewhat during the 1986 eruption [*McNutt et al.*, 1991].

4.5. Fuego, Guatemala and Arenal, Costa Rica

[33] To further generalize the result that tremor is well described by an exponential model we present data from Fuego and Arenal volcanoes. Figures 6c–6d shows these distributions with their fits to the exponential model.

[34] The tremor analyzed at Fuego was recorded following a VEI 2 explosive eruption during which an estimated 1×10^6 m^3 of tephra was erupted. Data were recorded on a helicorder from station FGO, 6 km southeast of the vent [*Yuan et al.*, 1984]. The dominant tremor frequency was 1 Hz. The correlation coefficients for the power law and

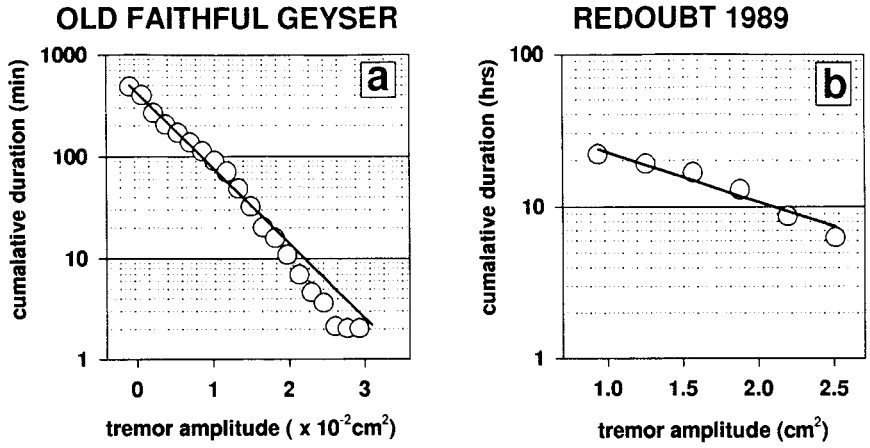

Figure 7. Duration-amplitude distributions for (a) seismic noise recorded in 1972 near Old Faithful Geyser, Yellowstone National Park and (b) the 13–14 December 1989 low-frequency swarm at Redoubt.

exponential models at Fuego are 0.83 and 0.99, respectively (Table 1).

[35] Tremor amplitudes and durations at Arenal were measured directly from helicorder records. Four days of tremor from April 1993 were examined and amplitudes were measured once per minute. Data were from a temporary station 2.3 km south of the vent. The tremor was associated with the continuous effusion of a block andesite lava flow, punctuated with periodic Strombolian explosions. A comparison of the correlation coefficients for the fits of the exponential and power law models shows again that the duration-amplitude distribution is better described with the exponential model (Table 1).

4.6. Old Faithful Geyser, Yellowstone National Park, Wyoming

[36] The seismicity at geysers has been used as an analog for volcanic seismicity [*Kieffer*, 1984; *Kedar et al.*, 1996]. Old Faithful geyser provides an isolated source of geothermal noise and an excellent data set to examine the duration-amplitude distribution. The same method of measuring tremor durations and amplitudes was applied to 8 hours of "geothermal noise" recorded on a small aperture array with an average distance of 50 m from Old Faithful geyser. Using a scale, duration-amplitude measurements were made from amplitude data published by *Iyer and Hitchcock* [1974, Figure 7]. The duration-amplitude distribution is shown in Figure 7a with a fit to the exponential model. As with the tremor, the geyser noise also is better fit with an exponential model (R^2 = 0.99) rather than a power law model (R^2 = 0.95; Table 1). The characteristic amplitude is 0.003 cm^2, which is smaller than all the volcanic cases and hence is the smallest of all the cases studied (Table 2).

4.7. Redoubt, Alaska

[37] At Redoubt, we examined the duration-amplitude distribution for a nontremor sequence. Durations and amplitudes were measured from RSAM data collected during the 24-hour swarm of low-frequency events preceding the 15 December 1989 eruption. This swarm initially consisted of large (M > 1.0) long-period events, which occurred more frequently in time over the next 19 hours until they coalesced into high amplitude tremor. The average amplitudes then began to decline at the time of the transition between individual events and continuous tremor [*Power et al.*, 1994]. The magnitude distribution for the located long-period events was uniformly distributed from the detection threshold to M = 1.4 and does not fit the Gutenberg-Richter distribution [*Lahr et al.*, 1994]. The swarm culminated in a phreato-magmatic eruption with a volume of 1.0–3.3 $\times$ 10^5 m^3 DRE and sent a plume to greater than 10 km above sea level [*Scott and McGimsey*, 1994].

[38] The duration-amplitude distribution is shown in Figure 7b with a fit to the exponential model. As with the tremor, the low-frequency swarm is better fit with an exponential model (R^2 = 0.95) rather than a power law model (R^2 = 0.88; Table 1). The characteristic amplitude is 1.4 cm^2, which is smaller than all eruptive tremor studied but greater than the noneruptive tremor and the geothermal noise at Old Faithful (Table 2).

5. Is Volcanic Tremor a Series of Low-Frequency Events Closely Spaced in Time?

[39] Using the general result of this study, exponential scaling of the duration-amplitude distribution of tremor, we now test an accessory hypothesis; tremor is composed of a series of low-frequency events closely spaced in time [e.g., *Fehler*, 1983]. This hypothesis comes from the observation that low-frequency events sometimes occur with an increasing rate until they grade into continuous tremor. Continuous tremor has also been observed to decay in episodic bursts of low-frequency events [e.g., *Koyanagi et al.*, 1987]. Further, the spectral features of tremor and low-frequency events can be very similar [e.g., *Fehler*, 1983]. The frequency-size statistics for some sequences of low-frequency events have been shown to exhibit power law scaling [e.g., *Minakami*, 1960; *Shimozuru and Kagiyama*, 1989; *Nishimura*, 1995].

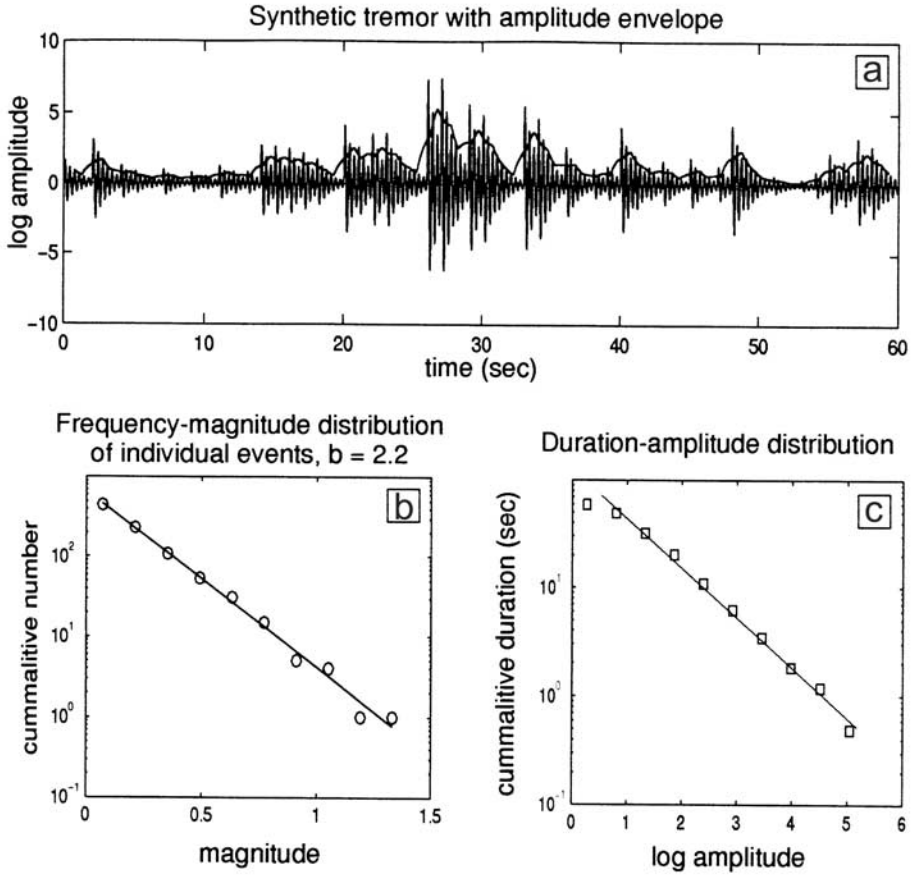

Figure 8. (a) Typical synthetic tremor created by summing a series of low-frequency events closely spaced in time. The black line shows a sliding average of absolute value of the synthetic tremor amplitude. (b) The frequency-magnitude distribution of the individual low-frequency events (b-value = 2.2) composing the synthetic tremor. (c) The duration-amplitude distribution calculated for the synthetic tremor. The linear relation, on this log-log plot, suggests power law-scaling.

Hence, if volcanic tremor is the superposition of many low-frequency events, then it should also exhibit power law scaling [*Nishimura*, 1995]. Two approaches are used to test this hypothesis. First, the duration-amplitude distribution is examined using a series of synthetic low-frequency earthquakes, and second, using an analytical examination of a low-frequency earthquake amplitude envelope function.

[40] A synthetic time series resembling volcanic tremor may be created by summing many low-frequency events closely spaced in time. The synthetic seismograms for low-frequency events are approximated by

$$\dot{u}_i(t) = \begin{cases} 0 & t < t_{i0} \\ A_i e^{\left(i\omega t - \frac{(t-t_{i0})}{\tau}\right)} & t \geq t_{i0} \end{cases} \quad (4)$$

where A_i is the amplitude of the ith event, ω is the event frequency (e.g., $\omega = 2\pi * 3$ Hz), τ is a decay constant (τ = 0.9 s), and t_{i0} is the time of the event onset. The events were randomly arranged in time, using a Poisson distribution for the inter-event spacing. We drew low-frequency earthquake amplitudes (A_i) from two distributions, a power law and a normal population. For the power law distribution, a range of scaling parameters or "b-values" were tested from 0.5 to 5, and, for the normal population, several mean amplitudes and standard deviations were tested.

[41] Figure 8 shows a typical example of the synthetic time series (Figure 8a), the frequency-magnitude distribution for low-frequency events (Figure 8b), and the resulting duration-amplitude distribution (Figure 8c). A power law distribution was obtained with a relatively high b-value (b = 2.2) which is commonly observed for low-frequency events near volcanoes [e.g., *Endo et al.*, 1981]. The average amplitude is plotted superimposed on the synthetic time series (Figure 8a). The durations and amplitudes are then measured and displayed in Figure 8c. The plot of log duration versus log amplitude (Figure 8c) shows a linear relationship corresponding to power law scaling for the duration-amplitude distribution. Similar results are obtained when the input parameters were varied (e.g., b-value, inter-event spacing, and decay constant).

[42] Low-frequency events at some volcanoes have been observed to occur only in a narrow band of magnitudes (e.g., Redoubt [*Lahr et al.*, 1994] and Pinatubo [*Ramos et al.*, 1996]). For this reason, synthetic runs were conducted

using normally distributed amplitudes for the low-frequency events. The resulting tremor duration-amplitude distributions were irregular and neither the power law nor the exponential model fit these distributions.

[43] The results from these synthetic time series tests show that exponential duration-amplitude scaling cannot be reproduced through the superposition of many low-frequency events closely spaced in time if the distributions of the low-frequency events obey a power law. Note that even though the synthetic seismogram itself has an exponential form (equation (4)), the power law distribution of event sizes dominates the scaling.

[44] We now show that the exponential scaling of the duration-amplitude distribution is not simply an artifact of our measurement technique on an exponentially decaying waveform such as the coda of a low-frequency earthquake. This demonstration also bears on the argument that tremor is a superposition of many low-frequency events.

[45] The amplitude envelope of a low-frequency earthquake can be approximated by a simplified version of equation (4)

$$A(t) = A_o e^{-\alpha t} \tag{5}$$

where A is the amplitude at time t, A_0 is the maximum amplitude to the earthquake, and α is a constant related to the attenuation. This represents a simple decay as is commonly observed in the coda of earthquakes. Duration-amplitude measurements similar to those made on tremor can be made on the envelope function by solving equation (4) as a function of A, as given below

$$t(A) = \frac{1}{\alpha} \ln\left(\frac{A_0}{A}\right), \tag{6}$$

In this case the duration of the signal at a given amplitude is $t(A)$ and the duration-amplitude distribution is formed by plotting this function. An inspection of the curve plotting log duration ($t(A)$) versus amplitude shows a nonlinear relation and therefore is not a candidate to produce the exponentially scaled duration-amplitude distribution. This test also suggests that the exponential duration-amplitude scaling cannot be reproduced through the superposition of many low-frequency events closely spaced in time, consistent with the results above.

6. Discussion

[46] The above case studies show clearly that an exponential scaling model, not a power law, provides a preferred description of the duration-amplitude distribution for volcanic tremor. The exponential model differs from the power law model primarily in that the exponential model requires the source process to be scale bound, not scale invariant. In other words, the amplitude variations of tremor are distributed about a constant characteristic amplitude. We suggest that the physical significance of the characteristic amplitude is that it is related to a constant feature of the tremor source, and we explore several possibilities. The discussion is related to indirect features of the data, and hence, is somewhat speculative.

[47] The scaling law for volcanic explosion earthquakes was recently examined by *Nishimura and Hamaguchi* [1993], and provides some insight. They compared the seismic energy of tectonic earthquakes with a relation derived for the kinetic energy of ejecta for volcanic explosions. The two equations are of similar form, and involve the fault length cubed (L^3) and stress drop for earthquakes, and correspondingly, the crater radius cubed (R^3) and pressure for explosions. For earthquakes, the stress drop is constant, so the seismic energy is scaled by the fault length. (Further, the ratio between the fault area and slip is constant, and this feature is preserved across all event sizes and is an expression of the scale invariance, which is related to the power law distribution.) For volcanic explosions, the pressure is constant, and the kinetic energy is scaled by the crater radius. We suggest that tremor has a volume source, similar to explosions, so the fundamental physics are similar; tremor and explosions often share frequencies and other wave characteristics. By analogy with earthquakes, the two possibilities to alter the scaling for explosions or tremor are to change the crater radius or the pressure. Thus, two basic classes of features providing a scaling bound on the amplitude of tremor are considered: 1) fixed source geometry with variable excess pressures, or 2) constant excess pressure and variable source geometries. For purposes of discussion these are treated as end-members although they may be interrelated.

[48] Field observations of exhumed dikes provide evidence for a fixed geometric dimension associated with the tremor source. *Chouet et al.* [1987] noted that dike widths have a fixed average value for a given area with a relatively small standard deviation. For example, the average width is 4 m for Iceland, 1.8 m for Scotland, 6 m at the Columbia River [*Williams and McBirney*, 1979], and 0.5 m at Kilauea [*Swanson et al.*, 1976]. Field observations have also shown that repeated eruptions can occur through the same vent and show very little or no modification of the vent (e.g., Pavlof [*McNutt et al.*, 1991] and Mt. Spurr [*Miller et al.*, 1995]). These fixed dimensions may provide a geometrical scaling constraint or bound on the tremor source. For many cases, the dominant period of shallow tremor appears fixed, independent of its amplitude, suggesting that the source size does not change, but the force (e.g., excess pressure) that drives the tremor source does [*Fehler*, 1983; *Chouet et al.*, 1987].

[49] For deep tremor at Kilauea, *Aki and Koyanagi* [1981] observed a positive correlation between tremor period and amplitude. They interpret this observation as a constant excess pressure that drives a crack, generating tremor, that is independent of the source size. The variations in amplitude are interpreted to be caused by a distribution of crack sizes. This model may be appropriate for deep tremor, because pressure fluctuations are likely to be small compared with the large overburden. Note that Kilauea tremor is the only deep tremor sample analyzed; all others are from shallow sources.

[50] A similar correlation between tremor period and amplitude has been observed for shallow tremor at Arenal volcano, Costa Rica [*Benoit and McNutt*, 1997]. Benoit and McNutt describe the tremor source at Arenal as a vertically oriented 200–600 m long resonator that is likely to be a gas-charged, magma-filled conduit. A source mechanism

similar to Kilauea may be occurring at Arenal, that is, a constant excess pressure is driving the tremor source and the source dimension (length) is changing. Alternatively, variable excess pressures may excite a relatively constant length resonator. Significant length changes seem unlikely; however, changes in the acoustic velocity of a resonator can be accomplished rather easily. For example, a velocity change corresponding to a 75% change in tremor frequencies can result from a 5 parts-per-thousand decrease in the gas fraction within the magma. Degassing processes may also contribute to changing pressure. We deduce that the pressure changes because the flow changes from low and steady (background) to high and intermittent (the explosions); the Bernoulli effect implies systematic pressure variations. However, the source location remains fixed within the same conduit occupying the upper few hundred meters of the volcano. Therefore, the Arenal case supports the hypothesis that the size (e.g., length) of the tremor source is constant and the pressure driving it is varying.

[51] The tensile strength of the wall rock or a solidified magma plug may also give an upper bound to the size of the tremor. If pressures exceed the strength of the surrounding rock, then brittle fracture may dominate the source process. At this point the scaling character of the tremor should change significantly, such as a change in slope of the duration-amplitude distribution or a change to a power law distribution. Such a break in scaling at large amplitudes was not observed for the cases examined in this study. All of the cases, however, are from relatively small eruptions, and the strength of the wall rock may not have been exceeded. To observe this effect, tremor associated with large eruptions must be recorded on-scale in the near field. To our knowledge, on-scale continuous recordings of eruption tremor from very large eruptions (VEI $\geq$ 4) do not yet exist. Future studies will benefit from the installation of modern high-dynamic-range broadband seismic instrumentation near explosive volcanoes capable of large eruptions.

[52] In summary, our data support the hypothesis that exponential scaling of tremor amplitudes is caused by a fixed source geometry driven with variable excess pressures. This implies that the inverse of the duration-amplitude distribution or the characteristic amplitude (λ^{-1}) is proportional to a geometric dimension of the source. For shallow tremor sources, these dimensions may be related to factors such as the distance between the bubble nucleation front or fragmentation front and the magma surface, or the average length of cracks or conduits.

[53] Characteristic amplitudes were calculated for case studies with the appropriate instrumental information. These varied from 7.7 cm^2 to 3×10^{-3} cm^2 reduced displacement (Table 2). The largest characteristic amplitude was recorded for deep tremor at Kilauea and the smallest was measured for geothermal noise at Old Faithful. The two smallest characteristic amplitudes for volcanoes are observed in association with hydrothermal activity. The seismic signals produced from Old Faithful are unambiguously associated with the boiling of groundwater within a conduit 22–175 m long [*Kieffer*, 1984]. The October 1992 Spurr noneruptive tremor episodes exhibited banding, which is interpreted as a cyclic interaction between a heat source (magma) and water [e.g., *McKee et al.*, 1981a; *Kieffer*, 1984; *McNutt*, 1992]. Furthermore, the volcano was emitting large quantities of steam, but no ash, at this time, providing additional evidence for the hydrothermal origin of the tremor. The December 1989 low-frequency swarm at Redoubt also had a relatively small characteristic amplitude. There was a phreatic component to the following eruption. This swarm has been interpreted as being caused by the interaction of groundwater with magmatic gases, steam and water driving a fixed crack ($280-380 \times 140-190 \times 0.05-0.20$ m) at a stationary point throughout the swarm [*Chouet et al.*, 1994]. We suggest that, in general, tremor of hydrothermal origin will have smaller characteristic amplitudes than tremor of magmatic origin. Two main factors lead to this outcome, smaller source dimensions (cracks and conduits within a hydrothermal system) and the intrinsically limited ability of hydrothermal boiling to generate strong tremor [*Leet*, 1988].

[54] The characteristic amplitudes for shallow tremor at Kilauea, eruptive tremor at Spurr and both Pavlof cases are similar, 2.3–5.6 cm^2 for volcanic activity that spans fissure eruptions, lava fountaining, and sub-Plinian eruptions (Table 2). It seems quite remarkable that such a wide variety of activities would exhibit similar characteristic tremor amplitudes. It is possible that similar source sizes exist for all of these cases. Perhaps, the conduit dimensions or the (vertical) distances between features such as the bubble nucleation or fragmentation front and the magma's surface are similar for each of these cases. The characteristic amplitude for deep tremor at Kilauea (7.7 cm^2) is somewhat greater than that for the shallow eruptive tremor studied. This difference suggests either that different processes are generating the tremor, or that the average source dimension is larger for the deep tremor.

[55] Spurr eruption tremor (Figure 3) and Pavlof (Figure 6a) both show breaks in the scaling at low amplitudes, corresponding to distinct characteristic scale lengths. In each of these cases the lowest amplitude tremor show a greater slope or smaller characteristic amplitude. We suggest that low amplitude tremor that is generated through hydrothermal or gas transport processes contributes to these distributions, and that at greater amplitudes tremor is associated only with magmatic processes. *Leet* [1988] suggested a similar explanation for the maximum amplitude of tremor associated with the 7 August and 16–18 October 1980, eruptions of Mount St. Helens. Unfortunately, absolute amplitude units were not available for the Karkar and Ulawun tremor data. Nonetheless, clear differences exist in the slopes of the tremor plots from Karkar and Ulawun (Figure 5). The characteristic amplitude for tremor associated with the magmatic eruptions is greater than the tremor associated with the phreatic explosions. Thus, all three cases show the same polarity; greater characteristic amplitudes for magmatic processes. The noneruptive tremor at Mt. Spurr shows a break in scaling at $\sim$4 cm^2, above which tremor durations decrease rapidly (Figures 2a and 3). We suggest that this scaling change represents an upper amplitude bound for tremor generated through hydrothermal processes.

[56] Exploiting these differences in the characteristic amplitudes could provide a useful method to improve the remote monitoring of volcanoes. Real-time measurement

and monitoring of this parameter may provide a simple discriminant between eruptive and noneruptive or hydrothermally generated tremor. This could be especially important at remotely monitored volcanoes where visual or other observations are difficult to obtain.

7. Conclusions

[57] In conclusion, we have shown that the duration-amplitude distribution of volcanic tremor is well described by an exponential function, not a power law as noted for earthquakes. This observation holds for 8 different volcanoes and 1 geothermal area, and is associated with a range of different volcanic phenomena. This type of amplitude scaling suggests that the tremor generating process is scale bound. We propose that exponential scaling of tremor amplitude is caused by a fixed source geometry driven by variable excess pressures. This implies that the inverse of the duration-amplitude distribution, or the characteristic amplitude (λ^{-1}), is proportional to a geometric dimension of the source. There are variations in the characteristic or mean amplitude for tremor associated with different types of volcanic activity. The strongest differences appear to be between tremor associated with magmatic and phreatic activity. This difference may provide a useful monitoring discriminant between tremor associated with magmatic and phreatic eruptions.

[58] The exponential scaling of tremor demonstrates that tremor source processes are fundamentally different from those of earthquakes. Finally, we have provided a fundamental observational constraint with which future theoretical tremor source models must be reconciled.

Appendix A: Definition of Reduced Displacement

[59] The reduced displacement is the root-mean square (RMS) ground displacement corrected for geometrical spreading. It has units of distance * amplitude or cm^2, and is thus a measure of the intensity or strength of the tremor source that can be used to compare intensities of tremor sources at different volcanoes. The normalizing factors depend on the types of seismic waves, body or surface waves, which are predominantly carrying the energy.

[60] The body wave reduced displacement is defined as [*Aki and Koyanagi*, 1981]:

$$D_R = \frac{A}{2\sqrt{2}} \cdot \frac{r}{M} \tag{A1}$$

The surface wave reduced displacement is defined as [*Fehler*, 1983]:

$$D_R = \frac{A}{2\sqrt{2}} \cdot \frac{\sqrt{r\lambda}}{M} \tag{A2}$$

where A is the peak-to-peak ground displacement, r is the distance between source and receiver, M is the instrument magnification, and λ is the wavelength.

[61] **Acknowledgments.** We thank A. Jolly, E. Brodsky, L. Mastin, R. Hansen and G. Beroza for their comments, which have improved this manuscript. We also thank two anonymous reviewers for their suggestions on an earlier draft of the paper. This work was supported by the Alaska Volcano Observatory under the U.S. Geological Survey Volcano Hazards and Geothermal Studies Program, and by additional funds from the State of Alaska.

References

Aki, K., Earthquake mechanism, *Tectonophysics*, *13*, 423–446, 1972.

Aki, K., and R. Y. Koyanagi, Deep volcanic tremor and magma ascent mechanism under Kilauea, Hawaii, *J. Geophys. Res.*, *86*, 7095–7109, 1981.

Bath, M., Earthquake magnitude—Recent research and current trends, *Earth Sci. Rev.*, *17*, 315–398, 1981.

Benoit, J. P., and S. R. McNutt, New constraints on source processes of volcanic tremor at Arenal volcano, Costa Rica, using broadband seismic data, *Geophy. Res. Lett.*, *24*, 449–452, 1997.

Chouet, B., R. Y. Koyanagi, and K. Aki, Origin of volcanic tremor in Hawaii, 2, Theory and discussion, in *Volcanism in Hawaii*, edited by R. W. Decker, T. L. Wright, and P. H. Stauffer, *U.S. Geol. Surv. Prof. Pap.*, *1350*, 1259–1280, 1987.

Chouet, B. A., R. A. Page, C. D. Stephens, J. C. Lahr, and J. A. Power, Precursory swarms of long-period events at Redoubt Volcano (1989–1990), Alaska: Their origin and use as a forecasting tool, *J. Volcanol. Geotherm. Res.*, *62*, 95–135, 1994.

Endo, E. T., and T. Murray, Real-time Seismic Amplitude Measurement (RSAM): A volcano monitoring and prediction tool, *Bull. Volcanol.*, *53*, 533–545, 1991.

Endo, E. T., S. D. Malone, L. L. Noson, and C. S. Weaver, Locations, magnitudes, and statistics of the March 20–May 18 earthquake sequence, in *The 1980 Eruptions of Mount St. Helens, Washington*, edited by P. W. Lipman and D. R. Mullineaux, *U.S. Geol. Surv. Prof. Pap.*, *1250*, 93–107, 1981.

Fehler, M., Observations of volcanic tremor at Mount St. Helens volcano, *J. Geophy. Res.*, *88*, 3476–3484, 1983.

Gutenberg, B., and C. F. Richter, Magnitude and energy of earthquakes, *Ann. Geofis.*, *9*, 1–15, 1954.

Hartmann, W. K., Terrestrial, lunar, and interplanetary rock fragmentation, *Icarus*, *10*, 201–213, 1969.

Ishimoto, M., and K. Ida, Observations sur les seismes enregistres par le microsismographe construit dernierement (in Japanese with French abstract), *Bull. Earthquake Res. Inst. Univ. Tokyo*, *17*, 443–478, 1939.

Iyer, H. M., and T. Hitchcock, Seismic noise in Yellowstone National Park, *Geophysics*, *39*, 389–400, 1974.

Kanamori, H., and D. L. Anderson, Theoretical basis for some empirical relations in seismology, *Bull. Seismol. Soc. Am.*, *65*, 1073–1095, 1975.

Kedar, S., B. Sturtevant, and H. Kanamori, The origin of harmonic tremor at Old Faithful geyser, *Nature*, *379*, 708–711, 1996.

Kieffer, S. W., Seismicity at Old Faithful Geyser: An isolated source of geothermal noise and possible analogue of volcanic seismicity, *J. Volcanol. Geotherm. Res.*, *22*, 59–95, 1984.

Korvin, G., Fractured but not fractal: Fragmentation of the Gulf of Suez basement, *Pure Appl. Geophys.*, *131*, 289–305, 1989.

Koyanagi, R. Y., B. Chouet, and K. Aki, Origin of volcanic tremor in Hawaii, 1, Data from the Hawaiian Volcano Observatory 1969–1985, in *Volcanism in Hawaii*, edited by R. W. Decker, T. L. Wright, and P. H. Stauffer, *U.S. Geol. Surv. Prof. Pap.*, *1350*, 1221–1257, 1987.

Koyanagi, R. Y., W. R. Tanigawa, and J. S. Nakata, Seismicity associated with the eruption, in *The Eruption of Pu'u O'o Eruption of Kilauea Volcano, Hawaii: Episodes 1 Through 20, January 3, 1983, Through June 8, 1984*, edited by E. W. Wolfe, *U.S. Geol. Surv. Prof. Pap.*, *1463*, 183–235, 1989.

Lahr, J. C., B. A. Chouet, C. D. Stephens, J. A. Power, and R. A. Page, Earthquake classification, location, and error analysis in a volcanic environment: Implications for the magmatic system of the 1989–1990 eruptions at Redoubt volcano, Alaska, *J. Volcanol. Geotherm. Res.*, *62*, 137–151, 1994.

Leet, R. C., Saturated and subcooled hydrothermal boiling in groundwater flow channels as a source of harmonic tremor, *J. Geophys. Res.*, *93*, 4835–4849, 1988.

Lindquist, K. G., J. P. Benoit, and R. A. Hansen, Near-real-time monitoring on a network of seismic stations with IceWorm: Automatic alarms for and spectral signals of the 1996 eruptions of Pavlof Volcano (abs.), *Seismol. Res. Lett.*, *68*, 332, 1997.

McKee, C. O., D. A. Wallace, R. A. Almond, and B. Talai, Fatal hydroeruption of Karkar volcano in 1979: Development of a maar-like crater, in *Cooke-Ravian Volume of Volcanological Papers*, edited by R. W. Johnson, *Geol. Surv. P. N. G. Mem.*, *10*, 63–84, 1981a.

McKee, C. O., R. A. Almond, R. J. S. Cooke, and B. Talai, Basaltic pyroclastic avalanches and flank effusion from Ulawun volcano in 1978, in *Cooke-Ravian Volume of Volcanological Papers*, edited by R. W. Johnson, *Geol. Surv. P. N. G. Mem.*, *10*, 153–165, 1981b.

McNutt, S. R., Observations and analysis of B-type earthquakes, explosions, and volcanic tremor at Pavlof Volcano, Alaska, *Bull. Seismol. Soc. Am.*, *76*, 153–175, 1986.

McNutt, S. R., Volcanic tremor at Pavlof volcano, Alaska, October 1973–April 1986, *Pure Appl. Geophys.*, *125*, 153–175, 1987.

McNutt, S. R., Volcanic tremor, in *Encyclopedia of Earth System Science*, vol. 4, 417–425, Academic, San Diego, Calif., 1992.

McNutt, S. R., T. P. Miller, and J. J. Taber, Geological and seismological evidence of the increased explosivity during the 1986 eruptions of Pavlof volcano, Alaska, *Bull. Volcanol.*, *53*, 86–98, 1991.

McNutt, S. R., G. Tytgat, and J. Power, Preliminary analyses of volcanic tremor associated with the 1992 eruptions of Crater Peak, Mt. Spurr, Alaska, in *The 1992 Eruptions of Crater Peak Vent, Mt. Spurr Volcano, Alaska*, edited by T. E. C. Keith, *U.S. Geol. Surv. Bull.*, *2139*, 161–178, 1995.

Miller, T. P., C. A. Neal, and R. B. Waitt, Pyroclastic flows of the 1992 Crater Peak eruptions: Distribution and origin, in *The 1992 Eruptions Of Crater Peak Vent, Mt. Spurr Volcano, Alaska*, edited by T. E. C. Keith, *U.S. Geol. Survey Bull.*, *2139*, 81–87, 1995.

Minakami, T., Fundamental research for predicting volcanic eruptions, 1, Earthquakes and crustal deformations originating from volcanic activities, *Bull. Earthquake Res. Inst. Univ. Tokyo*, *38*, 497–544, 1960.

Mogi, K., Magnitude-frequency relation for elastic shocks accompanying fractures of various materials and some related problems in earthquakes, *Bull. Earthquake Res. Inst. Univ. Tokyo*, *40*, 831–853, 1962.

Neal, C. A., R. G. McGimsey, C. A. Gardner, M. L. Harbin, and C. J. Nye, Tephra-fall deposits from the 1992 eruptions of Crater Peak, Mount Spurr volcano, Alaska: A preliminary report on distribution, stratigraphy, and composition, in The 1992 Eruptions Of Crater Peak Vent, Mt. Spurr Volcano, Alaska, edited by T. E. C. Keith, *U.S. Geol. Surv. Bull.*, *2139*, 65–80, 1995.

Neal, J. T., A. M. Langer, and P. F. Kerr, Giant desiccation polygons of Great Basin playas, *Geol. Soc. Am. Bull.*, *79*, 69–70, 1968.

Nishimura, T., Estimation of Ishimoto-Ida's m-value for seismic sources included in volcanic tremor, *Bull. Volcanol. Soc. Jpn.*, *40*, 53–57, 1995.

Nishimura, T., and H. Hamaguchi, Scaling law of volcanic explosion earthquake, *Geophys. Res. Lett.*, *20*, 2479–2482, 1993.

Okubo, P. G., and K. Aki, Fractal geometry in the San Andreas fault system, *J. Geophys. Res.*, *92*, 345–355, 1987.

Power, J. A., J. C. Lahr, R. A. Page, B. A. Chouet, C. D. Stephens, D. H. Harlow, T. L. Murray, and J. N. Davies, Seismic evolution of the 1989–1990 eruption of Redoubt volcano, Alaska, *J. Volcanol. Geotherm. Res.*, *62*, 153–182, 1994.

Ramos, E. G., E. P. Laguerta, and M. W. Hamburger, Seismicity and magmatic resurgence at Mount Pinatubo in 1992, in *Fire and Mud Eruptions and Lahars of Mount Pinatubo, Philippines*, edited by C. G. Newhall and R. S. Punongbayan, pp. 387–408, Philipp. Inst. Volcanol. Seismol., Quezon City and Univ. Wash. Press, Seattle, 1996.

Scholz, C. H., The frequency-magnitude relation of microfracturing in rock and its relation to earthquakes, *Bull. Seismol. Soc. Am.*, *58*, 399–415, 1968.

Scott, W. E., and W. G. McGimsey, Character, mass, distribution, and origin of tephra-fall deposits of the 1989–1990 eruption of Redoubt volcano, south-central Alaska, *J. Volcanol. Geotherm. Res.*, *62*, 251–272, 1994.

Shimozuru, D., and T. Kagiyama, Some significant features of pre-eruption volcanic earthquakes, in *Volcanic Hazards*, *IAVCEI Proc.*, vol. 1, edited by J. H. Latter, pp. 504–512, Springer-Verlag, New York, 1989.

Simkin, T., Terrestrial volcanism in space and time, *Annu. Rev. Earth. Planet. Sci.*, *21*, 427–452, 1993.

Smith, D. K., and T. H. Jordan, The size distribution of Pacific seamounts, *Geophys. Res. Lett.*, *14*, 1119–1122, 1987.

Swanson, D. A., W. A. Duffield, and R. S. Fiske, Displacement of the south flank of Kilauea volcano: The result of forceful intrusion of magma into the rift zones, *U.S. Geol. Surv. Prof. Pap.*, *963*, 1–39, 1976.

Turcotte, D. L., *Fractals and Chaos in Geology and Geophysics*, 221 pp., Cambridge Univ. Press, New York, 1992.

Vogt, P. R., Volcano-spacing, fractures, and thickness of the lithosphere, *Earth Planet. Sci. Lett.*, *21*, 235–252, 1974.

Warren, N. W., and G. V. Latham, An experimental study of thermally induced microfracturing and its relation to volcanic seismicity, *J. Geophys. Res.*, *75*, 4455–4464, 1970.

Williams, H., and A. R. McBirney, *Volcanology*, 397 pp., W. H. Freeman, New York, 1979.

Wolfe, E. D., C. A. Neal, N. G. Banks, and T. J. Duggan, Geologic observations and chronology of the eruptive events, in *The Eruption of Pu'u O'o Eruption of Kilauea Volcano, Hawaii: Episodes 1 Through 20, January 3, 1983, Through June 8, 1984*, edited by E. W. Wolfe, *U.S. Geol. Surv. Prof. Pap.*, *1463*, 1–98, 1989.

Wyss, M., Towards a physical understanding of the earthquake frequency distribution, *Geophys. J. R. Astron. Soc.*, *31*, 341–359, 1973.

Yuan, A. T. E., S. R. McNutt, and D. H. Harlow, Seismicity and eruptive activity at Fuego volcano, Guatemala: February 1975–January 1977, *J. Volcanol. Geotherm. Res.*, *21*, 277–296, 1984.

V. Barboza, Observatorio Vulcanologico y Sismologico de Costa Rica (OVSICORI), Universidad Nacional Aptdo 2346-3000, Heredia, Costa Rica.

J. P. Benoit and S. R. McNutt, Geophysical Institute, University of Alaska Fairbanks, P.O. Box 757320, Fairbanks, AK 99775-7320, USA. (steve@giseis.alaska.edu)